

# A New Approach to Mass Measurements of UHECR: Horizontal Air Showers

E. Zas

*Departamento de Física de Partículas,  
Universidade de Santiago de Compostela, E-15706 Santiago, Spain.  
zas@fpaxp1.usc.es*

## **Abstract.**

The role of Horizontal Showers induced by cosmic rays is discussed in detail. A new approach to the calculation of the muon component in horizontal air showers induced by protons, heavier nuclei or photons is presented which allows a simple analytical evaluation of the muon density profiles at ground level. The results of the first application of these results to horizontal air showers detected at the Haverah Park Array by the recently started *Leeds-Santiago collaboration*, leading to important restrictions on composition at ultra high energies, are reported.

## INTRODUCTION

Inclined showers were observed in the 1960's by a number of experiments [1–4] and it was immediately realized that they were different from the ordinary vertical showers and they had to be due to penetrating particles. At high zenith angles the slant atmospheric depth to ground level is enough to absorb the early part of the shower that follows from the standard cascading interactions, both of electromagnetic and hadronic type. Only penetrating particles such as muons and neutrinos can traverse the atmosphere at high zeniths to reach the ground or to induce secondary showers deep in the atmosphere and close to an air shower detector.

The idea that it may be possible to detect high energy neutrinos produced both in the atmosphere or away from the earth was put forward by Markov in 1960 [5]. Horizontal Air Showers (HAS) were at the end of the decade suggested as a possible means [6] but it was soon realized that the inclined showers that had been detected were more likely due to secondary interactions of the high energy muons that were produced in ordinary cosmic ray showers at the top layers of the atmosphere. Indeed inclined shower rates in the shower size range between  $10^2$  and  $10^5$  particles have been shown to be consistent with atmospheric muon bremsstrahlung [7–9], which is the dominant mechanism for HAS.

From the early days of air shower measurements until now inclined showers have been present in many experiments [10] and have given a great deal of information.

The Haverah Park array detected very inclined showers of the highest energies which were interpreted as muons from "ordinary" cosmic rays (presumably protons or nuclei) [11]. In the 1980's it became apparent that one of the interests of HAS was the identification of the prompt muon component in the atmospheric muon spectrum, an issue that is not yet settled and bounds on muon-poor HAS were established [12]. The non-observation of horizontal or upcoming air showers by the fluorescence technique gave a limit to the diffuse high energy neutrino flux [13].

Later on in the 1990's the prospects for high neutrino detection became a reality with a number of projects under planning or construction and intense theoretical activity resulted in various neutrino production mechanisms being proposed and flux predictions estimated [14]. Bounds on HAS played a significant role constraining diffuse neutrino flux predictions from three different mechanisms: For the pioneering calculation of the diffuse neutrino flux expected from proton acceleration in Active Galactic Nuclei (AGN) by Stecker et al. [16]. For "top-down" scenarios which have been discussed at length by other speakers in this conference, namely the annihilation of a class of topological defects, superconducting cosmic strings [17]. Lastly for "neutrino messenger" models in which the Ultra High Energy Cosmic Ray (UHECR) are locally produced by an extragalactic flux of high energy neutrinos that interacts with massive relic neutrinos clustering around our galactic halo, which have also been discussed at this conference [18,19]. The muon-poor HAS bound from AKENO [12] has been used to constrain both proton acceleration in AGN [15] and the annihilation of superconducting cosmic strings [20] and the Fly's Eye bound [13] has been used to constrain neutrino messenger models [21].

Although air shower arrays played an important role in neutrino astronomy, the limits on diffuse neutrino fluxes suggested that at least in the 10 TeV to 10 PeV band these detectors were more likely to play a role in establishing the prompt muon component than in actually detecting high energy neutrinos [9]. The atmospheric muon spectrum however decreases rapidly as the muon energy rises and as a result HAS induced by muon bremsstrahlung become a small background for neutrino detection in the upper energy region of the spectrum. Detectors aiming at the EeV range of the cosmic ray spectrum and above can thus place important constraints on the UHE end of the not yet established neutrino spectrum. (Incidentally this is the case for the two ambitious projects to detect Fluorescence and Čerenkov light from satellites presented in this conference [22,23].) It was shown that the Pierre Auger detector [24], also discussed by other speakers at this conference, has a large effective volume to neutrino detection for zenith angles above  $60^\circ$  [25,26]. This capability, which nicely connects the UHECR observation to the UHE neutrino searches, was clearly dependent on the ability to separate those hypothetical neutrino induced showers at high zeniths from a background of inclined showers induced by protons, nuclei or photons.

The many difficulties involved in both detecting and analysing inclined showers with particle arrays have prevented their systematic use in the past. At detection level shower arrays using scintillator detectors were usually placed in the horizontal plane making them less efficient for horizontal incidence. Moreover the typical

array, also lying in a horizontal plane, presents a much reduced sampling area for near horizontal incidence. At the analysis level, when these showers are produced by nucleons or photons, the geomagnetic distortions of the particle density profiles prevent the use of conventional approach to the study of Extensive Air Showers (EAS) such as using the standard measurements of particle density at a fixed distance to shower axis (such as  $\rho(600)$ ). Data analysis requires comparisons of measurements and expected particle density profiles. The brute force simulation of these shower profiles would demand very lengthy runs and much storage space which would make the data analysis extremely cumbersome. This approach was possibly too complicated to be justified when the first HAS were being recorded, particularly as shower models were quite primitive.

Understanding the cosmic ray background to neutrino detection by large air shower arrays was the original motivation of the study that is described in this article. The approach of using existing data from the Haverah Park array was proposed as a possible way to perform this study which had the clear advantage that new ideas about HAS could be immediately tested with real data. Haverah Park data had other specific advantages. The water Čerenkov detectors involved were rather deep and large which makes them more suitable for detecting horizontal events than scintillators. The signal deposited in them by charged particles is proportional to their tracklength so that muons that typically traverse the whole tank produce larger signals than photons or electrons. Muons constitute the dominant part at ground level of a photon, proton or nucleus induced shower at high zenith angles so again water Čerenkov tanks are at an advantage when detecting inclined showers. Lastly the Haverah Park array can be considered as a kind of prototype of the Auger observatory now under construction in Argentina. The proposal led to the Leeds-Santiago collaboration which has recently published the first analysis of inclined showers for zeniths above  $60^\circ$  induced by cosmic rays at energies above  $10^{19}$  eV [27].

The ability to analyse inclined showers above  $60^\circ$  induced by nucleons or photons essentially doubles the acceptance of any Air Shower array and opens a part of the sky that was previously inaccessible to the detector, besides establishing the background for neutrino detection. It was a pleasant surprise to find that on top of these obvious advantages these showers really provide a new tool for UHECR interpretation because they are probing muons of significantly higher energies than vertical showers. This tool has been shown to be very sensitive to composition when combined with vertical shower measurements and relevant conclusions have already been obtained from the analysis of the HAS observed at Haverah Park.

## **AZIMUTHAL SYMMETRY IN AIR SHOWERS**

The standard way to analyse EAS assumes circular symmetry for the average particle densities at ground level. There is little doubt that this is an accurate symmetry for vertical showers in the atmosphere in the absence of geomagnetic

effects. Indeed the symmetry principle lies behind the standard method for estimating the primary energy of an air shower through the relation between primary energy and the particle density at a given distance to shower axis, usually 600 m ( $\rho(600)$ ) which was demonstrated to be fairly independent of shower fluctuations and composition [28]. Even the existence of such a parameter obviously relies on an implicit assumption about circular symmetry.

However it was recently pointed out that deviations from symmetry exist and that they become important for correctly estimating the primary energy of events particularly for zeniths above  $50^\circ$  [29,30]. The circular symmetry is broken by the magnetic field and for inclined showers also by the density gradient in the atmosphere. Clearly particles having transverse (to the shower axis) momenta  $p_\perp$  pointing upwards will develop showers in a thinner density atmosphere than those with  $p_\perp$  pointing downwards. Neither of these effects is however very important at low zenith angles. The gradient induced asymmetry is expected to be small at all angles in the plane perpendicular to shower axis. The lateral spread of a shower, of order the Molière radius ( $10 \text{ g cm}^{-2}$ ), corresponds to very small differences in matter depth travelled by particles in the upper and lower sides of the shower plane when compared to the total travelled depth.

Inclined showers are different from vertical showers in that the hadronic and electromagnetic parts of the shower have been completely developed and absorbed before reaching the ground. There is however a penetrating component of the shower mostly muons and neutrinos from pion decays that reaches the ground. As a result the muons in the front are produced rather high in the atmosphere, at sites which are physically rather distant from the observation plane at ground level. The approach chosen for the study of inclined showers consists of eliminating the effect of the Earth's magnetic field. The study of showers in the absence of the earth's magnetic field maintains the circular symmetry and hence has enormous advantages for the study of the relations between the particle densities at ground and all cosmic ray relevant variables such as primary energy, zenith angle, composition and extrapolations of the relevant interactions. If the effects of the magnetic field can be implemented *a posteriori* that is once the lateral structure of the shower is known, the process of calculating particle densities at ground level would become a great deal simpler. This has enormous advantages at the levels of event simulation, of understanding the physical origin of the inclined shower features and of fitting experimental results to theory.

## MUON SHOWERS

Consider a shower muon of an inclined shower produced high in the atmosphere at a distance  $d$  to ground level and reaching ground level at a distance  $r$  to shower axis in a plane transverse to the shower axis as schematically shown in Fig. 1. This muon has an energy  $E$  sufficiently high to reach ground level and let us assume that it has a transverse momentum  $p_\perp$  that is small compared to  $E$ . In the absence

of magnetic fields the muon travels to ground in a straight line. If we assume that the start of the muon track is right on the shower axis then clearly  $r$  is related to  $d$ ,  $p_{\perp}$  and to  $p$  (or  $E$ ) through:

$$r = \frac{p_{\perp}}{p} d \simeq \frac{cp_{\perp}}{E} d. \quad (1)$$

For inclined showers both  $p_{\perp}$  and  $d$  in Eq. 1 have distributions. It is not difficult to conclude that the  $d$  distribution is narrow compared to the value of  $d$ . The majority of the muons are produced in a relatively narrow depth interval corresponding to the shower maximum for the parents (mostly pions that have average energy 25% larger than  $E$ ). This range is of order a few radiation lengths, say  $200 \text{ g cm}^{-2}$  while the distance  $d$  is controlled by the atmospheric slant depth from the production site to the ground which is over 3800 (10,000)  $\text{g cm}^{-2}$  for showers with zenith angles above  $75^{\circ}$  ( $85^{\circ}$ ). The  $p_{\perp}$  distributions on the other hand has an average of order 200 MeV/c. The value of  $d$  sets the scale of the problem because it controls the matter depth from the production site to the ground and thus determines the minimum energy that a muon needs to reach the ground before losing its energy. Clearly as the zenith angle rises both  $d$  and the average muon energy must also rise. The average values and the standard deviations of  $d$  are shown in Table 1

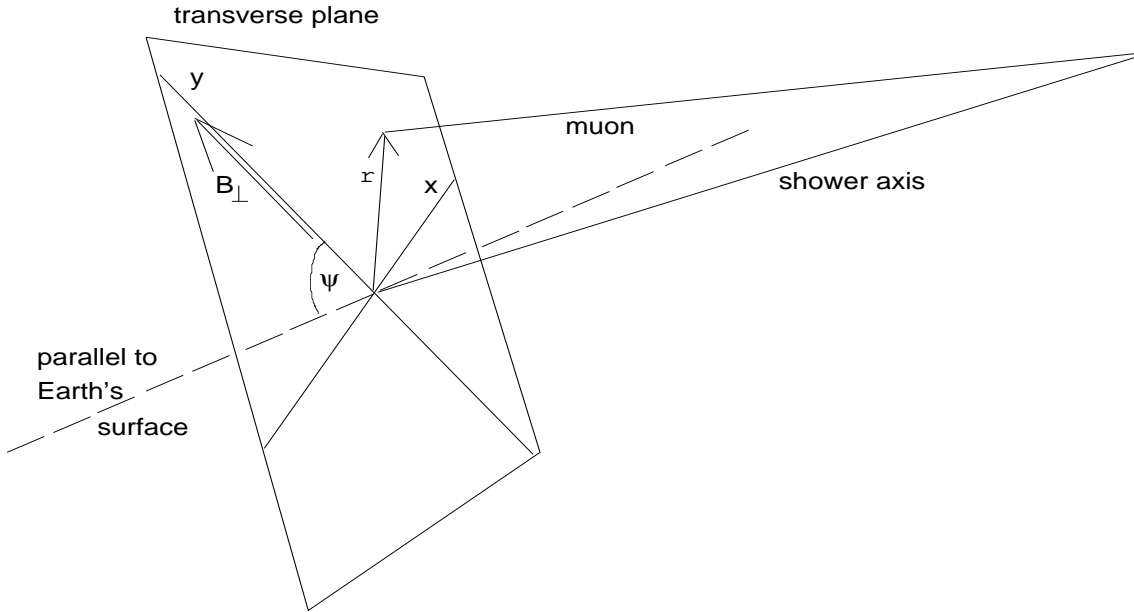


**FIGURE 1.** The plane perpendicular to the shower axis or *transverse plane* and some useful geometrical definitions for Horizontal Air Showers. The  $y$  axis is chosen along the direction of  $B_{\perp}$  which is the projection of the magnetic field onto the transverse plane.  $\psi$  is the angle subtended by the  $y$  axis and the intersection of the transverse and the ground planes.

$\theta$ (degrees)	d (km)	$\Delta d$ (km)	$\langle E \rangle$ (GeV)	$N_\mu \times 10^{-6}$	$\Delta N_\mu \times 10^{-6}$
0°	3.9	2.8	8.1	29.	6.5
60°	16	6.5	18.9	13.3	2.4
70°	32	10	32.9	7.8	1.4
80°	88	17	77	3.3	0.7
87°	276	31	204	1.2	0.2

**TABLE 1.** Relevant parameters for muon production as obtained in 100 proton showers of energy  $10^{19}$  eV with a relative thinning of  $10^{-6}$  simulated with AIRES using SIBYLL 1.6 cross sections. Average values and RMS deviations for production altitude ( $d$ ), muon energy at production ( $\langle E \rangle$ ), and total number of muons at ground level ( $N_\mu$ ).

together with the average muon energy at production and the average number of muons at ground level for different zeniths.

If one takes  $d$  and  $p_\perp$  to be fixed Eq. 1 implies that the energy spectrum and the lateral distribution of the muons are dependent. If either function is known the other can be deduced from it. The approximation of fixing  $d$  and  $p_\perp$ , crude as it seems, can be used to reproduce the lateral distribution in a wide range of distances to the shower axis from the energy spectrum of the muons. One needs to fix the distance  $d$  to the average values obtained in simulations and  $p_\perp$  to a value  $\simeq 200$  MeV/c.

Eq. 1 with fixed  $p_\perp$  and  $d$  also implies a particularly important anticorrelation between muon energy and distance to shower axis in the transverse plane. This anticorrelation shows up in the simulations of inclined showers very clearly as illustrated by the plot of the average muon energy as a function of  $r$  shown in Fig. 2. The error bars in the graph indicate the standard deviations of the muon energy distributions.

Deviations of the muon tracks by the Earth's magnetic field ( $\vec{B}$ ) can be easily implemented by assuming that the muons are bent in a helix type trajectory which can be approximated by the arc of a circle. For small deviations only the projection of  $\vec{B}$  onto the transverse plane,  $\vec{B}_\perp$ , matters. As a result it can be easily shown that the deviation of the muon in the transverse plane,  $\delta x$ , is at right angles to  $\vec{B}_\perp$  and given by:

$$\delta x = R \left[ 1 - \sqrt{1 - \left(\frac{d}{R}\right)^2} \right] \simeq \frac{d^2}{2R} = \frac{eB_\perp d}{2p}, \quad (2)$$

where  $e$  is the electron charge and  $p$  is the muon momentum and we have expanded brackets to first order. For  $\delta x$  less than 2 km we expect it to be valid at the 5% level at zenith  $60^\circ$  because the typical production distance  $\langle d \rangle$  is 16 km. At higher zenith the approximation is excellent.

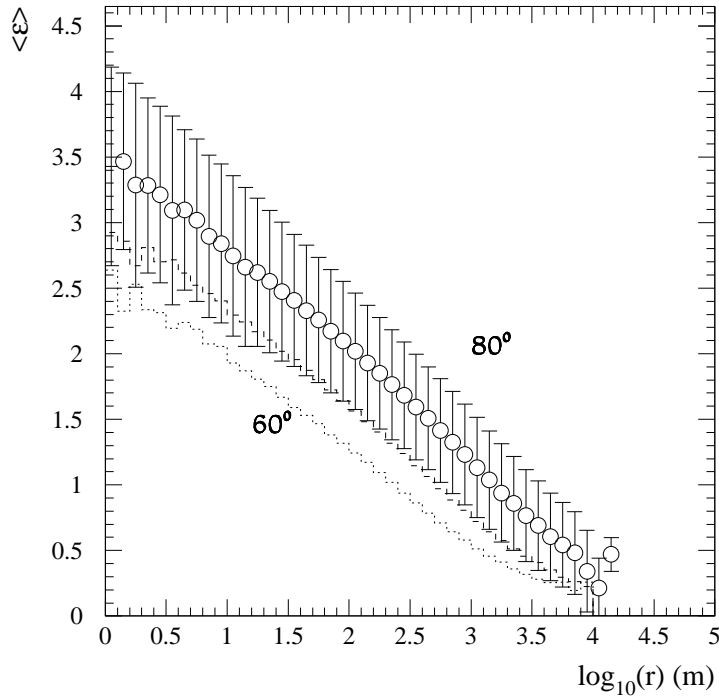


**FIGURE 2.** Correlation between  $\langle \epsilon \rangle = \langle \log_{10} E_\mu \rangle$  and  $\log_{10} r$  for zenith angles  $60^\circ$ ,  $70^\circ$ , and  $80^\circ$  from bottom to top, see text. Error bars show the width of the  $\epsilon$  distribution for  $80^\circ$ .

When we combine the above relation with Eq. 1 we obtain the following expression:

$$\delta x = \frac{e|B_\perp|d^2}{2p} = \frac{0.15|B_\perp|d}{p_\perp} \bar{r} = \alpha \bar{r}, \quad (3)$$

where in the last equation  $B_\perp$  is to be expressed in Tesla,  $d$  in m and  $p_\perp$  in GeV. This expression is telling us that all positive (negative) muons that, in the absence of a magnetic field, would fall in a circle of radius  $\bar{r}$  around shower axis, are translated a distance  $\delta x$  to the right (left) of the  $\vec{B}_\perp$  direction. The dimensionless parameter  $\alpha$  measures the relative effect of the translation. When  $\alpha \ll 1$  the magnetic effects are very small. However when  $\alpha > 1$  the magnetic translation exceeds the deviation the muons have due to their  $p_\perp$ . In this case *shadow* regions with no muons are expected in the muon density profiles. For an approximate  $p_\perp \sim 200$  MeV/c and  $B_\perp = 40 \mu\text{T}$  this happens when  $d$  exceeds a distance of order 30 km, that is for zeniths above  $\sim 70^\circ$ . These shadow regions in the transverse plane are indeed an outstanding feature of the ground density profiles at high zeniths.

It turns out that a very accurate description of the ground density profiles can be obtained using these simple ideas, provided one allows for an energy distribution of the muons at a fixed distance to shower axis, which has an average given by Eq. 1. Simulations have shown that a log normal distribution is adequate, or equivalently

that  $\epsilon = \log_{10} E$  is assumed to be distributed with a gaussian of width  $\sim 0.4$ . The values of other inputs needed for calculating densities at each zenith angle such as the effective distance travelled by muons  $d$ , their lateral distribution function, and the average muon energy as a function of distance to shower axis are taken from simulations without magnetic field using AIRES [31]. It is a straightforward calculation to convert the radial distribution functions in the absence of a magnetic field to density patterns when the field is turned on, using the first equality in Eq. 3 and the corresponding coordinate transformation. Details of this method and extensive checks are given in Ref. [32].

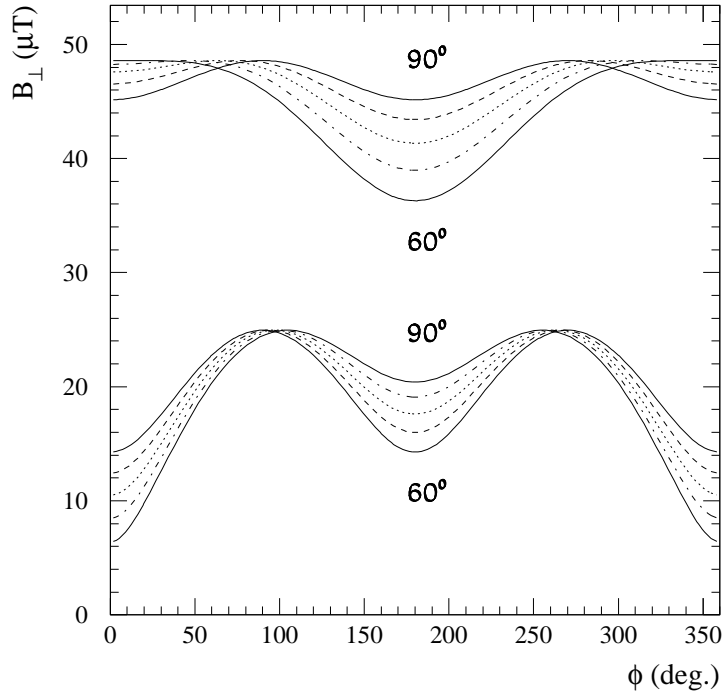


**FIGURE 3.** Magnetic field projection onto the transverse plane as a function of azimuthal angle for the Haverah Park location (top lines) and Pampa Amarilla (bottom lines). Lines are for zenith angles  $60^\circ$ ,  $70^\circ$ ,  $80^\circ$ ,  $87^\circ$ , and  $90^\circ$ .

The particle densities in the transverse plane only need to be converted to the ground plane. It is remarkable that the relevant component of the magnetic field is its projection onto the transverse plane,  $\vec{B}_\perp$ . This projection in principle depends on the azimuthal direction of the shower and can be very different depending on the local orientation of the magnetic field vector, or equivalently on the array site location. Besides the magnitude of the magnetic field it is in fact the vertically upward component that is responsible for many of these quantitative differences between sites. The direction of  $\vec{B}_\perp$  in the transverse plane changes as the azimuthal

angle of the incident shower is changed. Depending on the site under consideration the changes in magnitude and direction of  $\vec{B}_\perp$  as the incident azimuthal angle is varied can be very important. As an example this is illustrated in Fig. 3 where the magnitude of  $\vec{B}_\perp$  is plotted as a function of azimuth for two different site locations, that of Haverah Park and that of *Pampa Amarilla* where the southern hemisphere Auger observatory is being constructed, more details can be found in [32].

## CHARACTERIZATION OF INCLINED SHOWERS

The approach described in the previous two sections has allowed a lot of progress in analysing existing data on HAS. Technically it allows the separation of azimuthal effects from other effects that are more interesting from the physics point of view. Systematic studies have been made of the changes in the transverse density patterns as the primary energy, zenith angle and composition of the cosmic ray is changed and the results are also very enlightening.

The effect of zenith angle has already been discussed. As the zenith angle rises the distance travelled by the muons  $d$  and their energy  $E$  rises. This makes inclined showers rather different from the vertical ones and, since  $d$  changes by over a factor 10 between  $60^\circ$  and  $90^\circ$ , it also implies that  $85^\circ$  showers are very different from  $70^\circ$  showers. As the zenith angle is increased the muons that are sampled at the ground have increasingly higher energies, and thus relate to earlier stages in shower development. Inclined showers are probing the shower core and the Earth's magnetic field is acting as a spectrometer for these high energy muons.

Once the zenith angle is fixed there is little that changes from shower to shower and the effect is spectacular for showers of a given composition once the interaction model is fixed. As the energy of the primary proton changes, to an excellent approximation, the muon lateral distribution in the absence of a magnetic field has a universal shape. As a result it can be described by a single parameter, the normalization or equivalently the total number of muons in the shower. This effect is illustrated in Fig. 4 showing the lateral muon distribution for different zenith angles and a range of energies spanning the interval  $10^{16} - 10^{19}$  eV. The situation is analogous for the two hadronic models used, QGSJET [33] and SIBYLL [34].

The result is not surprising after all. The scaling in showers has been known for a very long time and reflects the fact that the distributions are governed by the low energy physics that affects the majority of the shower particles. Besides the total number of particles, the main difference in showers of different energy is the position of shower maximum. It is well known that shower maximum only varies logarithmically with shower energy and this is a relatively small change when compared to the distance  $d$  travelled by the muons in HAS. Once the muons are produced they are not very much affected until they reach ground level and as a result only the total number of muons produced matters to a very good approximation. This is in contrast to vertical showers where arrays are also measuring the electromagnetic contribution that, after reaching shower maximum becomes expo-

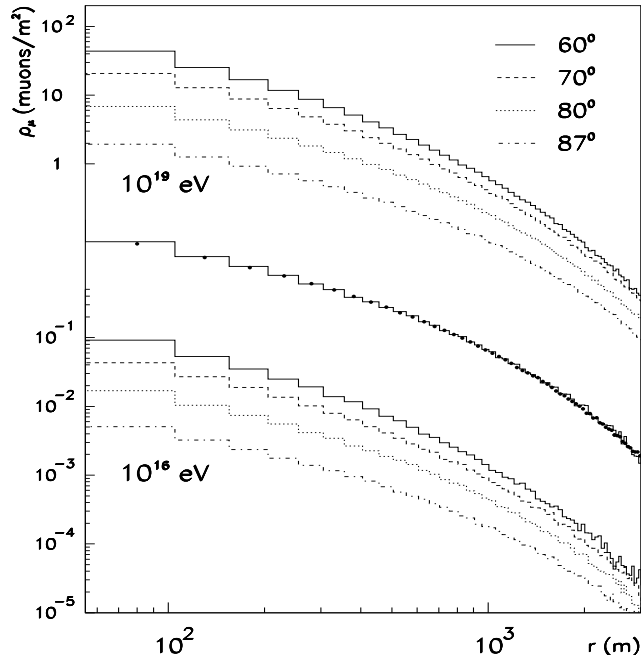


**FIGURE 4.** Lateral distribution functions for primary protons of energy  $10^{16}$ ,  $10^{17}$ ,  $10^{18}$  and  $10^{19}$  eV using SIBYLL.

nentially attenuated with depth and thus the densities observed at ground level are very sensitive to the position of shower maximum.

For showers initiated by a heavy nucleus the situation is analogous and moreover the resulting lateral distribution is also extremely similar to that of protons. The explanation is the same since, besides the normalization, the main difference between the muons in proton and heavy ion showers is again the depth of maximum. For each zenith angle we thus characterize the shower by the total number of muons. The total number of muons in proton showers is shown in Fig. 5 as a function of primary energy for the SIBYLL hadronic model. The results can be easily parameterized by a function of the following type:

$$N = N_{\mu} E^{\beta} \quad (4)$$

where  $\beta$  is a constant for a given model and mass composition as shown in Table 2.

In the case of photons the lateral distributions are also quite independent of primary energy with the exception of showers affected by the LPM effect. But the LPM effect is a density effect and is thus less important for horizontal than for vertical showers. Moreover the interactions of high energy photons with the Earth's magnetic field effectively imply that a high energy photon can be considered as a bunch of lower energy photons that are less likely to be affected by the LPM effect. The density profiles of the muons produced by photon primaries are similar to those produced by protons but the agreement is not as good as between protons and heavy nuclei because the dominant shower interactions are different. Photon

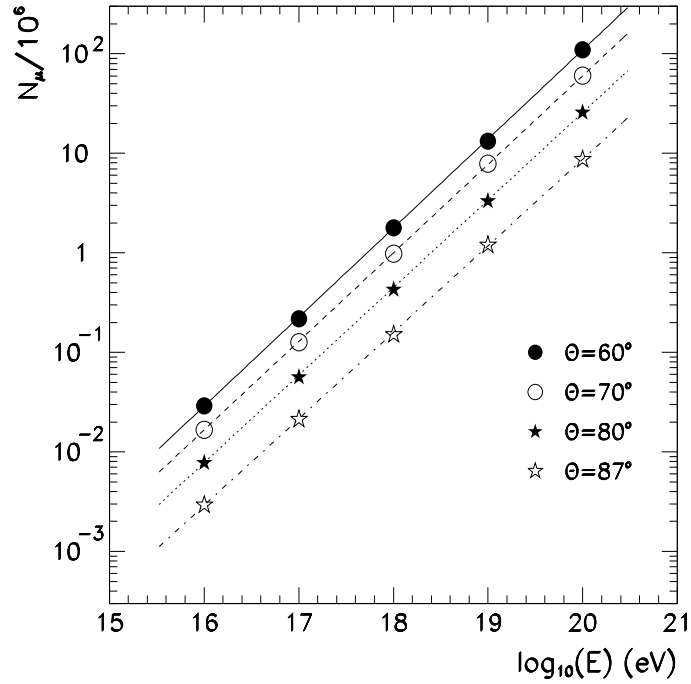


**FIGURE 5.** The relationship of total muon number to primary energy for protons of four zenith angles using the SIBYLL model.

showers are slightly narrower. To a relatively good approximation however the muon lateral distribution of photon showers can be assumed to be like that of protons with  $\beta = 1.2$  and with  $N_\mu(10^{19} \text{ eV}) = 5.7 \cdot 10^5$ . Although the rise of the number of muons with energy is more rapid for photon primaries than for proton, at  $10^{19} \text{ eV}$  photons are still 9 times poorer in muons than protons.

Model	A	$\beta$	$N_\mu (10^{19} \text{ eV})$
SIBYLL	1	0.880	$3.3 \cdot 10^6$
	56	0.873	$5.3 \cdot 10^6$
QGSJET	1	0.924	$5.2 \cdot 10^6$
	56	0.906	$7.1 \cdot 10^6$

**TABLE 2.** Relationship between muon number and primary energy for two hadronic models and two primary masses (see equation 4).

## INTERPRETATION OF HAS DATA

The ability to generate muon density profiles makes it possible to make rate simulations for a given array geometry and in particular that of Haverah Park with which nearly 10,000 events were recorded with zenith angles above  $60^\circ$  between 1974 and 1987. The Haverah Park detector was a  $12 \text{ km}^2$  air shower array using 1.2 m deep water Čerenkov tanks in Northern England and which has been described elsewhere [35]. For the study to be described the recorded data for zenith angle above  $60^\circ$  were reanalyzed for arrival direction for the described analysis using all the time information available for the tanks. This gave an improvement in angular accuracy.

The process of making this simulation is however rather elaborate because the signals in the detectors have to be carefully calculated. It is clear that signals in water Čerenkov tanks from muons close to the horizontal directions are rather different from vertical incidence. The shower muons are more energetic than in vertical showers and thus more likely to produce interactions in the tank which complicate the signal distributions. These corrections to the signal are discussed in detail in Ref. [36] where it is shown that the corrections due to delta rays, direct light going into the phototubes, the electromagnetic component due to muon decay and muon interaction processes in the tank (mostly pair production and bremsstrahlung) are of great importance and increase the rate by a factor between 3 and 4 with respect to a calculation using only the signal due to the muon tracks. The use of signal distributions becomes essential and these were calculated with WTANK [37], a program based on GEANT.

The measured trigger rate as a function of zenith angle is well reproduced in magnitude and azimuth when these corrections are carefully taken into account. The rate simulation can be made assuming different composition and/or different hadronic models and the results compared to the data. While protons slightly underestimate the rate, heavy nuclei overestimate it, so clearly a mixture of the two can reproduce the data for any of the two hadronic interaction models considered [36].

The fact that smooth average muon density profiles can be obtained with the described prescription allows the possibility of making fits to the data in an attempt to evaluate the energy and impact parameter of individual showers once a given composition is assumed. For zeniths below  $70^\circ$  a remnant electromagnetic contribution from the showering process is considered, which is concentrated near the shower core. The fitting process is complex because the Haverah Park array at large zenith angles only samples a small band in the transverse plane of the shower and uncertainties in arrival directions as well as correlations between fitted parameters have to be taken into account. To improve the fits additional information from an infilled portion of the array [38] that was running simultaneously part of the time was included when available.

The correlation between arrival direction and energy demands an iterative process in which the arrival directions are corrected once the core position is determined.

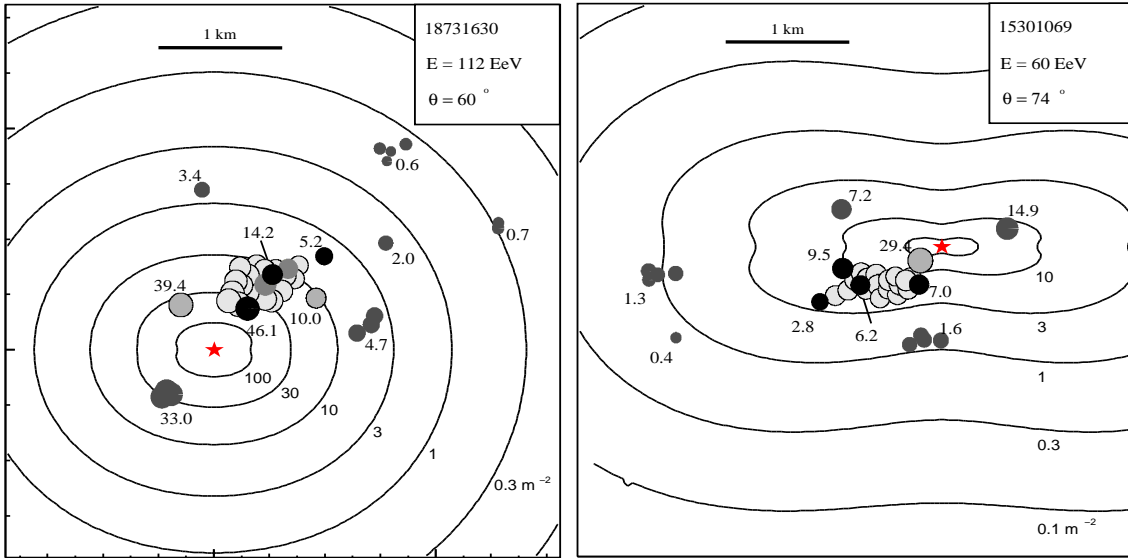


**FIGURE 6.** Density maps of two events in the plane perpendicular to the shower axis. Recorded muon densities are shown as circles with radius proportional to the logarithm of the density. The detector areas are indicated by shading; the area increases from white to black as 1, 2.3, 9, 13, 34  $\text{m}^2$ . The position of the best-fit core is indicated by a star. Selected densities are also marked. The y-axis is aligned with the component of the magnetic field perpendicular to the shower axis.

This refitting procedure for the arrival directions takes into consideration both the curvature corrections and the distribution of the arrival time of the first muon in terms of the signal received in the tanks. Once the first density fit is performed with the arrival directions obtained with a time fit to a plane front, the sequence of a time fit with curvature corrections and a density fit with the new arrival directions is repeated three times. Two examples of the results of such fits compared to the average density contours are shown in Fig. 6.

Once the data have been analysed a number of quality cuts are performed to eliminate badly reconstructed events. A cut has been taken selecting showers with shower core at a distance less than 2 km from the array center to make sure that the event is well contained within the array. A second cut has been made on the density fit rejecting those events that have a  $\chi^2$  probability below 1%. Lastly a cut has been made to reject events that have a large error in the energy determination which is defined to be the sum in quadrature of the error from the fit and the error due to the uncertainty in the arrival direction. This error is required to be below 50%: this automatically eliminates all showers with zenith angles above  $80^\circ$ . After these cuts are performed 2, 7 and 46 events are reconstructed with proton equivalent energies above  $10^{20}$  eV,  $4 \cdot 10^{19}$  eV and  $10^{19}$  eV, respectively.

The procedure is applied to the data and to simulation using the cosmic ray spectrum of reference [39]. The simulated data goes through an identical fitting procedure and the resulting rate is compared to measurement. The agreement between the integral rate above  $10^{19}$  eV measured and that obtained with simulation

is striking when the QGSJET model is used. Sibyll leads to a slight underestimate of the observed rate.

In the context of this conference what is of more importance is the new possibility that HAS open for studying composition at the highest energies. The universality of the muon lateral distribution function is very powerful and once the equivalent proton energy is determined for all events, the corresponding energies under the assumption that the primaries are iron nuclei (photons) can be obtained by multiplying the proton energy by a factor which is  $\sim 0.7$  (6) for  $10^{19}$  eV and which varies slowly with equivalent proton energy. As a result when a photon primary spectrum is assumed the simulated rate seriously underestimates the observed data by a factor between 10 and 20. A fairly robust bound on the photon composition at ultra high energies can be established assuming a two component proton-photon scenario. The photon component of the integral spectrum above  $10^{19}$  eV ( $4 \cdot 10^{19}$  eV) must be less than 41% (65%) at the 95% confidence level. Details of the analysis are presented in [27] and will be expanded elsewhere. A similar analysis can be made for a two component scenario with protons and iron nuclei. When the QGSJET model is used a similar limit restricting the iron component to less than 54% above  $10^{19}$  eV can be similarly established. In this case the iron only assumption leads to an overestimate of the rate. The limit obtained is however less robust in the sense that it is fairly sensitive changes in the interaction model and/or assumptions about the incident cosmic ray flux [27].

## CONCLUSIONS

I have summarized recent progress in understanding density patterns of Extensive Air Showers at high zenith angles performed by the Leeds-Santiago collaboration and which is described in detail in references [27,32,36].

I have reviewed a scheme for understanding the complex muon density patterns that develop at ground level because of the geomagnetic effects on the muon component of these showers. The scheme can be used as an effective parameterization of the average density profiles at ground level and simplifies the task of performing simulations to be compared with data.

The ideas have been successfully tested with the Haverah Park data and the measured rate is consistent with simulations. The recorded individual density patterns can be fitted to average values obtained in this scheme and the energy of the cosmic rays extracted for a given composition. The analysis of inclined air shower data from Haverah Park Array for energies above  $10^{19}$  eV has been shown to be consistent with a proton composition using the QGSJET model for hadronic interactions. As a result of this study the photon component of the UHECR spectrum at energies above  $10^{19}$  eV must be less than 41% with a 95% confidence level.

The detection of large HAS provides a new tool for the study of high energy cosmic ray which has been shown to be very sensitive to primary composition in the EeV range and above. The cosmic ray spectrum is measured by the detec-

tion of vertical showers in a composition independent fashion. For high zeniths particle arrays detect mostly intermediate energy muons at ground level and the measured rate becomes particularly sensitive to photon composition on the basis of the reduced muon content of photon induced showers. The analysis of such inclined showers can effectively double the aperture of any given extensive air shower detector array at these energies and particularly for the Auger Observatories now in construction. The prospects for establishing photon composition at EeV energies and above by such arrays are significantly enhanced using this method.

**Acknowledgements:** I thank A.A. Watson and R.A. Vázquez for suggestions after reading this manuscript. This work was supported in part by CICYT (AEN99-0589-C02-02) and by Xunta de Galicia (PGIDT00PXI20615PR).

## REFERENCES

1. T. Hara *et al.* *Proc. of the XI Int. Cosmic Ray Conf.*, Budapest (1969), *Acta Physica Academiae Scientiarum Hungaricae* 29, Suppl. 3, p. 125-131, (1970); Nagano, M. *et al.*, *J. Phys. Soc. Japan* **30** 33 (1971).
2. E. Böhm *et al.*, *Proc. of the XI Int. Cosmic Ray Conf.*, Budapest (1969), *Acta Physica Academiae Scientiarum Hungaricae* 29, Suppl. 3, p. 121-124, (1970).
3. Alexander, D. *et al.*, *Proc. of the XI Int. Cosmic Ray Conf.*, Budapest (1969), *Acta Physica Academiae Scientiarum Hungaricae* 29, Suppl. 3, p. 215, (1970).
4. D. Andrews *et al.* *Proc. of the XI Int. Cosmic Ray Conf.*, Budapest (1969), *Acta Physica Academiae Scientiarum Hungaricae* 29, Suppl. 3, p. 337-342, (1970).
5. M.A. Markov, in *Proc. of the Annual Conf. on High Energy Physics*, Rochester (1960), p. 578.
6. V.S. Berezinsky and G.T. Zatsepin, *Yad. Fiz.* **10** (1969) 1228. [*Sov. J. Nucl. Phys* **10** (1969) 696].
7. P. Kiraly *et al.*, *J. Phys. A: Gen. Phys.* **4** (1971) 367.
8. S. Mikamo *et al.*, *Lett. al Nuovo Cimento* **34** N 10, (1982) 273.
9. E. Zas, F. Halzen and R.A. Vázquez, *Astropart. Phys.* **1**, 297 (1993).
10. Yu.N. Antonov, Yu.N. Vavilov, G.T. Zatspin *et al.*, *Zh. Éksp. Teor. Fiz.* **32** (1957) 227 (*Sov. Phys. JETP* **5** (1957) 172).
11. A.M. Hillas *et al.*, *Proc. of the XI Int. Cosmic Ray Conf.*, Budapest (1969), *Acta Physica Academiae Scientiarum Hungaricae* 29, Suppl. 3, p. 533-538, (1970).
12. Nagano, M. *et al.*, *J. Phys. G: Nucl. Phys.* **12** 69 (1986);
13. R.M. Baltrusaitis *et al.*, *Phys. Rev.* **D 31**, 2192 (1985).
14. For a review see for instance, P. Bhattacharjee and G. Sigl, *Phys. Rept.* **327** (2000) 109-247, T.K. Gaisser, F. Halzen and T. Stanev, *Phys. Rept.* **238** (1995) 173, and references therein.
15. F. Halzen and E. Zas, *Phys. Lett.* **B289** (1992) 184-188; F. Halzen and E. Zas, In *Proc. of the High energy neutrino astrophysics*, Honolulu, World Sci., Singapore (1992), p 186-195.

16. F.W. Stecker, C. Done, M.H. Salamon and P. Sommers, *Phys. Rev. Lett.* **66** (1991) 2697; F.W.Stecker, M.H.Salamon *Space Sci. Rev.* **75** (1996) 341-355
17. P. Bhattacharjee *et al.*, *Phys. Rev. Lett.* **69** (1992) 567.
18. T.J. Weiler, *Astropart. Phys.* **11**, 303 (1999).
19. D. Fargion, B. Mele, and A. Salis, *Astrophys. J.* **517**, 725 (1999).
20. J.J. Blanco-Pillado, R.A. Vázquez, and E. Zas, *Phys. Rev. Lett.* **78**, 3614 (1997).
21. J.J. Blanco-Pillado, R.A. Vazquez, E. Zas, *Phys. Rev.* **D61** (2000) 123003.
22. B. Khrenov in these proceedings.
23. O. Catalano and L. Scarsi in these proceedings.
24. *The Pierre Auger Project Design Report.* By Auger Collaboration. FERMILAB-PUB-96-024, Jan 1996. 252pp.
25. G. Parente and E. Zas, in *Proceedings of the 7th Int.Symposium on Neutrino Telescopes.* p. 345, ed. by M. Baldo Ceolin, Venice (1996).
26. J. Capelle, J.W. Cronin, G. Parente, and E. Zas, *Astropart. Phys.* **8** (1998) 321.
27. M. Ave, J.A. Hinton, R.A. Vazquez, A.A. Watson, and E. Zas, *Phys. Rev. Lett.* **85**, (2000) 2244.
28. A.M. Hillas, D.J. Marsden, J.D. Hollows, and H.W. Hunter, in *Proc. of the XII Int. Cosmic Ray Conf.*, Hobart **3** (1971) 1001.
29. E.E. Antonov, L.G. Dedenko, Yu.P. Pyt'ev *et al.*, *Pis'ma Zh. Éksp. Teor. Fiz.* **68** (1998) 177 (*JETP Letts.* **68** (1998) 185).
30. A.A. Ivanov *et al.*, *Pis'ma Zh. Éksp. Teor. Fiz.* **69** (1998) 263 (*JETP Letts.* **69** (1999) 288).
31. AIRES: A System for Air Shower Simulation, S.J. Sciutto, *Proc. of the XXVI Int. Cosmic Ray Conf.* Salt Lake City (1999), vol. 1, p. 411-414; S.J. Sciutto, *preprint archive astro-ph/9911331*.
32. M. Ave, R.A. Vázquez, and E. Zas, *Astropart. Phys.* **14** (2000) 91.
33. N.N. Kalmykov and S.S. Ostapchenko, *Yad. Fiz.* **56** (1993) 105; *Phys. At. Nucl.* **56**(3) (1993) 346; N.N. Kalmykov, S.S. Ostapchenko, and A.I. Pavlov, *Bull. Russ. Acad. Sci. (Physics)* **58** (1994) 1966.
34. R.T. Fletcher, T.K. Gaisser, P. Lipari, and T. Stanev, *Phys. Rev.* **D50** (1994) 5710; J. Engel, T.K. Gaisser, P. Lipari, and T. Stanev, *Phys. Rev.* **D46** (1992) 5013.
35. R.M. Tennent, *Proc Phys Soc* **92** (1967) 622. M.A. Lawrence, R.J.O. Reid, and A.A. Watson, *J Phys G* **17** (1991) 733.
36. M. Ave, J.A. Hinton, R.A. Vazquez, A.A. Watson, and E. Zas, *Astropart. Phys.* **14** (2000) 109.
37. J.R.T. de Mello Neto, WTANK: A GEANT Surface Array Simulation Program GAP note 1998-020.
38. D M Edge *et al.* *Proc. of the XV Int. Cosmic Ray Conf.* (Plovdiv) vol. 9 (1977) p. 137.
39. M. Nagano and A.A. Watson, *Rev. Mod. Phys.* **72** (2000) 689.